Charles E. Glass,[1] *James R. Carr,*[2] *Hsien-Min Yang,*[3] *and Donald E. Myers*[4]

Application of Spatial Statistics to Analyzing Multiple Remote Sensing Data Sets

REFERENCE: Glass, C. E., Carr, J. R., Yang, H.-M., and Myers, D. E., "**Application of Spatial Statistics to Analyzing Multiple Remote Sensing Data Sets,**" *Geotechnical Applications of Remote Sensing and Remote Data Transmission, ASTM STP 967,* A. I. Johnson and C. B. Pettersson, Eds., American Society for Testing and Materials, Philadelphia, 1987, pp. 000-000.

ABSTRACT: The purpose of this paper is to present results from preliminary research using image spatial statistics to improve the resolution of low-resolution digital images. Improvement is needed whenever images from different sensors, and often when images from different spectral bands within the same sensor, are collected for geotechnical interpretation.

The experimental procedure involves degrading one of two digital images in adjacent spectral bands to simulate a low-resolution image. New samples within the sparse, low-resolution image are subsequently estimated using the spatial characteristics displayed in a variogram function and an estimation process known as co-kriging or co-estimation. The resulting high-resolution estimation image is compared with the original undegraded image as a check on estimation accuracy. Reconstruction accuracy, as judged by mean square error (MSE), improved from MSE = 826 for sample replication to 56 for co-kriging.

For cases where geotechnical decisions rely on accurate knowledge of image amplitudes, this research suggests that co-kriging provides an accurate and flexible estimation technique. Moreover, co-kriging appears to be a promising technique for future automated image interpretation and feature extraction algorithms.

KEY WORDS: remote sensing, image processing, geostatistics, image registration

The purpose of this paper is to present the results of preliminary research using image spatial statistics to improve the resolution of low-resolution images. Although advanced remote sensing systems, multispectral sensors, and satellite and airborne geophysics have contributed to improving the quality of geotechnical engineering practice, these same advances in data collection have also brought about a crisis in geotechnical data management and interpretation. Available to the geotechnical engineer today, for example, is a wide variety of valuable remote sensing and geophysical information. Use of this information, however, is restricted by fundamental limits on the capacity of the human brain to understand and process information from multiple sets of data. Experimental findings by Sagi and Julesz [*1*], for example, suggest that interpretation (knowing or deciding "what" something is) of even a single, simple feature on a single image requires time-consuming search by focal attention and serial processing. The brain uses parallel processing only for searching a data set for the location of a known target. Hence, interpreting even modest quantities of data can present an overwhelming task.

[1]Department of Mining and Geological Engineering, The University of Arizona, Tucson, AZ 85721.
[2]Department of Geological Sciences, Mackay School of Mines, University of Nevada, Reno, NE 65401.
[3]Department of Mining and Geological Engineering, The University of Arizona, Tucson, AZ 85721.
[4]Department of Mathematics, The University of Arizona, Tucson, AZ 85721.

Q6329D
pd
#8

Automated machine interpretation and computer-generated image understanding will eventually improve the speed and quality of human interpretation. However interpretation proceeds, whether solely by human efforts, or by some combination of computer and human expertise, some fundamental preprocessing of digital data is needed to ensure that data sets gathered by different sensors are registered, and that corresponding elements (pixel, or ground resolution elements) on all digital images relate to approximately the same area on the ground. Registration is usually a two-stage process. First, images are "warped" to conform to some standard image or base map. Second, new image elements are estimated to increase the effective resolution of sparse, lower-resolution data. In this paper we report on results of preliminary research into the effectiveness of applying spatial-statistics estimation techniques (co-kriging) to improve the resolution of sparse data sets (the second stage of image registration). The aim is to utilize information contained in high-resolution data to estimate new image elements in a low-resolution image. Low-resolution data typically might include thermal or passive microwave bands in satellite remote sensing systems, or generally low-resolution geophysical techniques such as gravity.

Procedure

The purpose of the experiment is to test the efficacy of a sample estimation technique that employs the tendency of neighboring data samples to be similar. The procedure is to select two high-resolution images from the same sensor in different, but adjacent, spectral bands. This selection ensures that the two data sets are registered. One image serves as a control image to guide the subsequent estimation; the second image is degraded using a low-pass filter. The degraded image is then subsampled by preserving only intermittent elements and intermittent lines. The resulting sparse image simulates a low spatial resolution image in which the value of each element represents an average of the original neighboring elements (Fig. 1). The deleted elements are subsequently reestimated using the high-resolution data in the control image to-

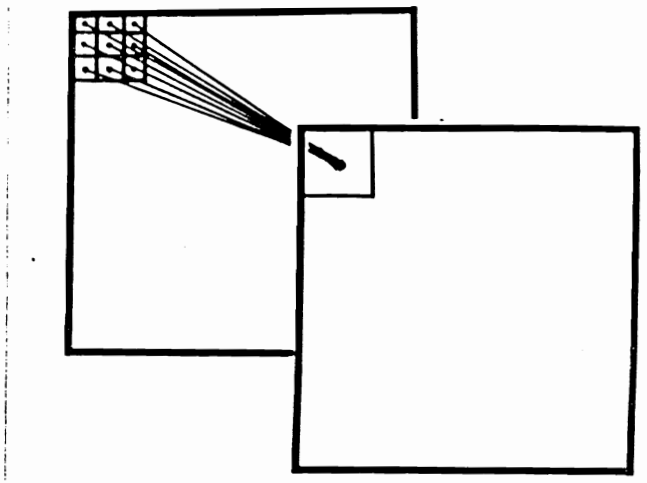

FIG. 1—*Schematic representing the procedure for image degradation. Low-pass filtering averages nine neighboring samples and replaces the central term with the average. Subsampling removes all but the central term in the window.*

gether with the sparse low-resolution data. This procedure permits the accuracy of the reconstruction to be estimated through comparison with the original undegraded image.

Experimental Work

Several procedures for increasing the sample density of sparse data have been reported. The procedure should be selected with an eye towards the ultimate purpose of the reconstruction. Images contain two fundamental types of information for geotechnical interpretation purposes: amplitude information, and texture information. The amplitude information is provided by the value of each digital image element. For many geotechnical purposes actual element amplitudes are less important than relative amplitudes within an image (the image histogram). This may explain the popularity and success of point-computer operations designed to improve image contrast by "stretching" the histogram of digital values in some desired way. In spectral ranges beyond the visible, such as the thermal and passive microwave regions, however, the element amplitudes carry important information related, for example, to thermometric temperature, moisture content, and in some cases pollution. In all cases where amplitude information is important, image estimation techniques should provide the best estimate possible for the missing data. Conventional techniques for interpolation include pixel replication and nearest neighbor interpolation [2], cubic convolution [3], and many others. All of these techniques rigidly assign weights to neighboring samples, thereby assuming spatial correlation among samples, without explicitly considering the degree of spatial correlation that exists. Thus, the weights to be used and the number of nearby samples to be considered in the estimation are specified using rules that are independent of the data.

Image texture information is contained in the abruptness with which sample values change within an image (image spectrum). Image texture yields information on geologic structure, stream pattern, and cultural conditions, and can be enhanced using filters. If image texture interpretation is the ultimate aim of image analysis, sample estimation may be only a secondary or intermediate step. Techniques to reconstruct image texture involve adding to an image the edges or frequency information derived from filtering a high-resolution image [4]. When perfect correlation exists between the high-resolution and low-resolution images, this procedure accurately reconstructs both textural and amplitude information. In data sets where low correlation between images is the rule (consider visible and thermal images, for example) this approach adds significant artifact to the reconstructed image because the correlation, or rather lack of correlation between images, is not considered in the technique.

The experimental work reported here investigates a way to use the within-image and between-image spatial correlation to estimate samples. The weighting scheme for the estimate depends upon the spatial correlation, making it possible to vary the weights not only for different sets of images, but within sets during the estimation process. The approach shows promise as a fundamental computer vision tool, because the decision to change weights can be made automatically by the computer during estimation.

The spatial correlation is the key, and can be represented in several ways. Early efforts relied on the joint-probability density function [5], which represents the relative frequency of occurrence of pairs of radiance values at two points in an image separated by some distance h. More recently the co-occurrence matrix [6] has been used to define spatial correlation for texture extraction. We suggest capturing the spatial correlation using a function called the variogram function [7]. The variogram function, equivalent to the spatial autocorrelation, computes the mean difference between samples separated by distance h, and is given by

$$\gamma(h) = \frac{1}{2N} \sum_{i=1}^{N} [Z(x) - Z(x + h)]^2 \tag{1}$$

In Eq 1, $Z(x)$ and $Z(x + h)$ are image brightness values, and N is the total number of sample pairs separated by h. The shape of the variogram function reflects the degree of correlation between samples. Variogram functions that rise as h increases indicate that the spatial correlation decreases as more distant samples are chosen, until a separation distance is reached at which knowledge of one sample tells us nothing about the others (uncorrelated).

The spatial structure of an image represented by the variogram can be used to estimate the value of image elements at unsampled locations. This estimate, Z^*, at point, x_0, known as the kriging estimate, is given by

$$Z^*(x_0) = \sum_{i=1}^{N} \lambda_i Z(x_i) \tag{2}$$

where N is the number of points located within a distance, R, of x_0, each $Z(x_i)$ is the value of a sample at the ith location, and λ is a vector of weights chosen using the variogram function to model the intersample spatial correlation. An estimate within a random set of samples (spatially uncorrelated), for example, would set N equal to the total number of samples and λ equal to $1/N$, which corresponds to using the mean value as the estimate. For random data the mean is as good as any other estimate. If the sample data are spatially correlated, however, a better estimate is achieved by considering nearby samples more important than distant samples. In such cases, λ is not a constant but depends upon the distance from the estimation point. The exact form chosen for λ depends on the variogram.

The cardinal idea is to use image spatial characteristics (as presented by the variogram function) of a high-resolution control image, together with the spatial characteristics of a low-resolution image, to specify the degree of cross-correlation existing in the two images. This cross-correlation is then used to increase the sample density of the low-resolution image by estimating new samples (regenerating or reconstructing the deleted samples).

This estimation process is known as co-kriging or co-estimation. Journel and Huijbregts [8] give some insight into the idea, but practical development has relied on our previous work presented in Carr et al. [9] and in Myers [10]. Like kriging, co-kriging is a weighted average, linear, unbiased estimator; yet unlike kriging, it can yield estimates of several variables simultaneously. This joint estimation process utilizes within-image sample autocorrelation and between-image sample cross correlation to improve estimation accuracy. We have specifically developed co-kriging for improving sparse, low-resolution data, and have previously applied the technique to earthquake ground motion estimation.

For co-kriging, Eq 2 is slightly modified to account for the multiple variable estimation, hence

$$\bar{Z}^*(x_0) = \sum_{j=1}^{N} \bar{Z}(x_j)\Gamma_j \tag{3}$$

where $\bar{Z}^*(x_0) = [Z_1^*(x_0), Z_2^*x_0), \ldots, Z_m^*(x_0)]$, m is the number of variables to be estimated at location x_0, N is the number of known data locations used in the estimation process, and the Z_m^* corresponds to different remotely sensed data sets.

Equation 3 is analogous to Eq 2 except that the estimate $\bar{Z}^*(x_0)$ is not a Scalar as in kriging (Eq 2), but rather is vector, the elements of which correspond to estimated variables in the different data sets. For example, the estimated vector at x_0 here will contain estimates of the reflectance at x_0 in the green and red spectral bands. The Γ is a matrix of weights. These weights depend upon the spatial correlation within each spectral band (autocorrelation), as does λ in Eq 2, but also depend upon the cross-correlation that exists between bands. Hence, image reconstruction using co-kriging requires m variograms and $m(m-1)/2$ cross-variograms for the estimation of m variables per location. To estimate high-resolution in a coarse-resolution image,

the estimation locations in the sparse data are chosen coincident with the sample locations of the high-resolution data.

To proceed, two images having high spatial resolution were chosen (Fig. 2). The two original images were collected using a visible near-infrared scanner (VNIR) at an altitude of 5000 m. The images were acquired as part of the National Aeronautics and Space Administration/Jet Propulsion Laboratory/Geosat (NASA/JPL/Geosat) project in 1983 [*11*]. Both images have a spatial resolution of 10 m. To simulate a low-resolution image, the digital data in Fig. 2*b* were filtered using a 3 × 3 low-pass convolution operator and subsampled so that only every third sample and every third line were retained (Fig. 3). Variogram functions were calculated for both images as shown in Fig. 4, and a cross variogram calculated as simply

$$\gamma_c(h) = \sum_N \{(Z_g(x) + Z_r(x) - [Z_g(x+h) + Z_r(x+h)]\}^2 \quad (5)$$

where $Z_g(h)$ and $Z_r(h)$ are sample values in the green and red images (Figs. 2*a* and 2*b*) respectively, and other symbols are defined in Eq 1.

The reconstructed image is shown in Fig. 5*a*, together with a full image generated by a simple sample replication in Fig. 5*b*. The image in Fig. 5*b* represents the most trivial sample estimation (simply repeating existing samples to increase sample density). Figs. 5*c* and 5*d* are enlargements of Figs. 5*a* and 5*b*, respectively, to show image structure more adequately. As a simple figure of merit to represent estimation accuracy, a mean square error (MSE) was calculated comparing the original red-band image and the reconstructed red-band image. The MSE for the kriged image is 187 compared with an MSE of 826 for the sample replication image. More sophisticated interpolation algorithms will naturally perform far better than the sample replication of Fig. 5*b*. As the interpolation weighting scheme approaches that of kriging, the results should become more similar, but the heuristic or rigid weighting schemes of standard interpolation algorithms will only approach, never surpass, the accuracy and flexibility provided by kriging.

Comparison of Figs. 5*a* and 2*b* shows that the reconstruction process has produced a smoother image than the original. The smoothness is due to two processes. First, although the co-kriging weights applied to the high-resolution control image are negative emphasizing edges, the weights applied to the low-resolution image are positive, tending to produce a smooth appearance even though high-resolution information has been added. (Please note the detail in Fig. 5*c* which is not contained in Fig. 5*d*.) Second, the reconstructed image has a lower contrast than does the original. To improve contrast the kriged image (ki) was further processed using sample values on the control image (ci). In Fig. 6*a* each sample of the kriged image was modified using

$$S_{new} = S_{ci} \times S_{ki} \quad (6)$$

and in Fig. 6*b* each sample has been altered by

$$S_{new} = \frac{SD_{ci}}{SD_{ki}} (S_{ki} - mean_{ki}) + mean_{ki} \quad (7)$$

In Eq 6 and Eq 7, SD is the standard deviation and S is the sample gray level value.

The MSEs of Figs. 6*a* and 6*b* are 56 and 175, respectively. The MSE between the two original images (original green and red bands) is 410, hence we are confident that the MSE improvement in the reconstruction is a reflection of the accuracy of the kriged image and not merely an artifact of the control image. Both modified images are more similar to the original, but still smooth. Following Schowengerdt's [*4*] lead, we increase the texture by filtering the control image with a high-pass (3 × 3) convolution filter and adding the results (edges or slope information) to the kriged image (Fig. 7). Although this image displays more texture than does Fig. 6*a*, the MSE has increased to 486. Hence it appears that this process has in effect added to the

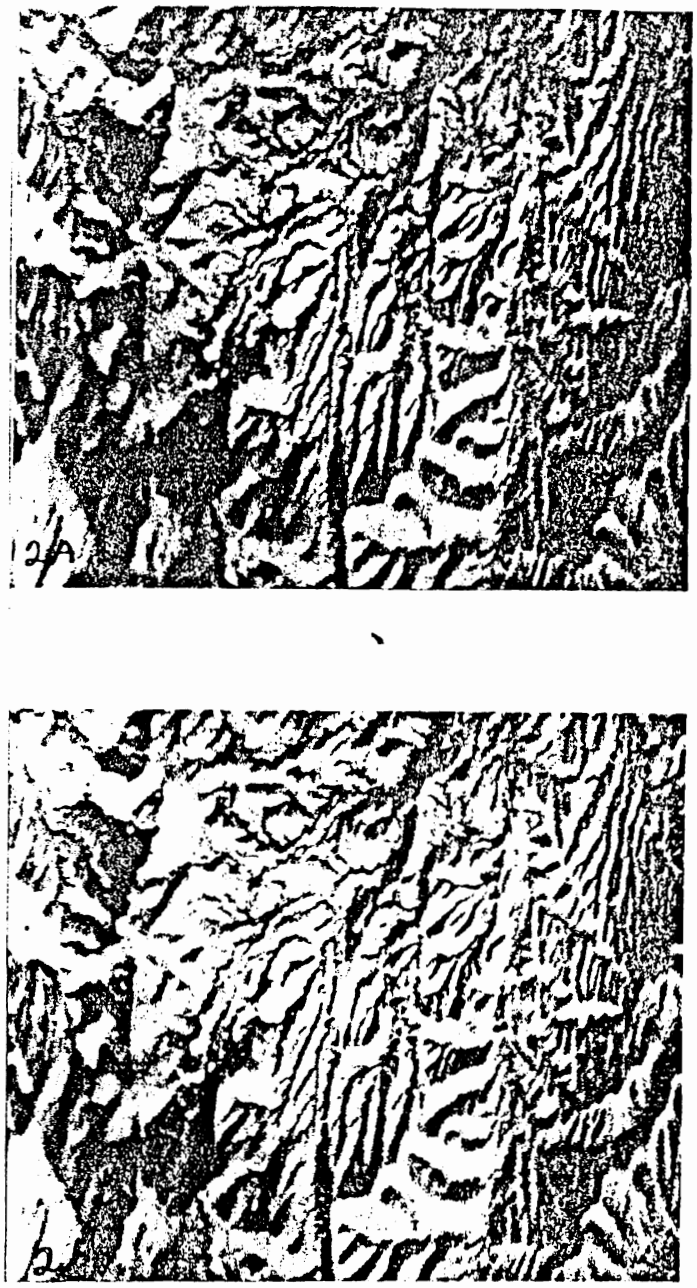

FIG. 2—*High-resolution images used for experimentation. Figure 2a corresponds to a green spectral band (wavelength = 0.52 to 0.60 μm), and Fig. 2b corresponds to a red spectral band (wavelength = 0.63 to 0.69 μm). These scenes were chosen because of their high texture content.*

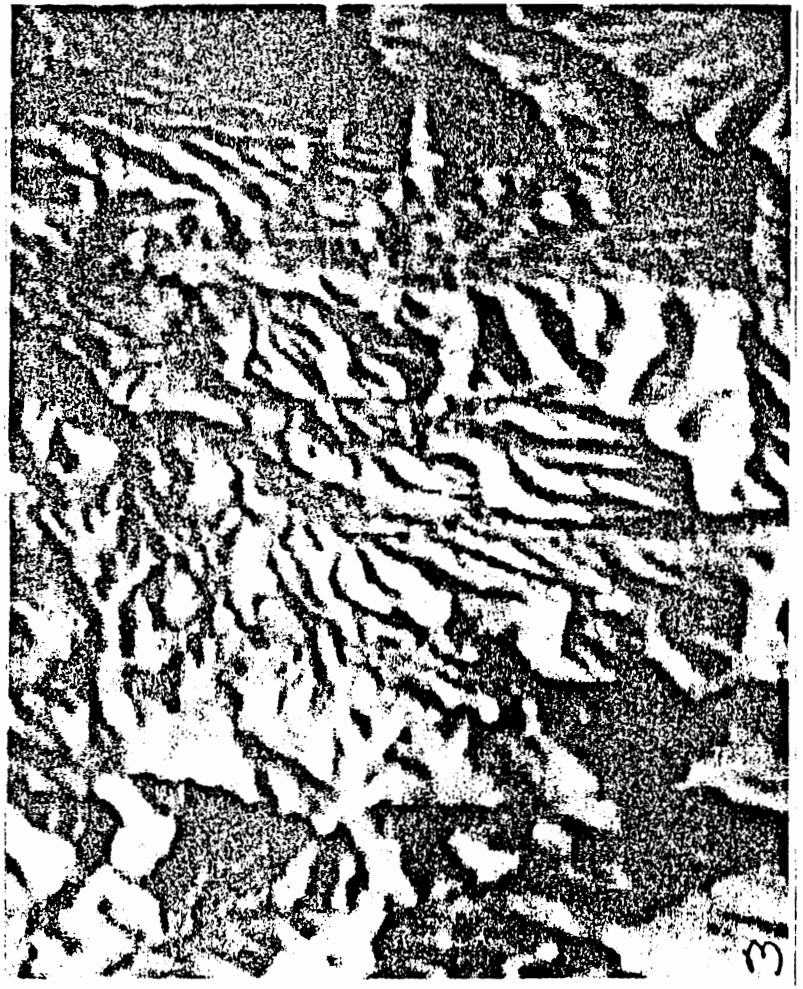

FIG. 3—*Simulated low-resolution image. Figure* 2b *has been degraded by filtering and subsampling. Although the image retains significant detail, the smoothing is quite obvious.*

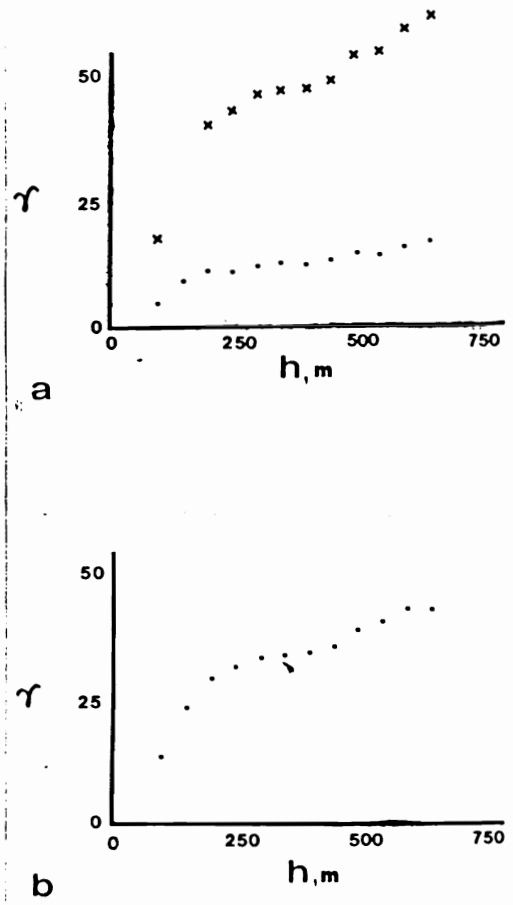

FIG. 4—*Variogram functions modeled using Figs.* 2a *and* 2b. *Figure* 4a *shows the variogram function for Fig.* 2a *(dots) and the cross variogram (x's) computed for both images. Figure* 4b *shows the variogram function computed using Fig.* 2b.

reconstructed error an artifact proportional to the original error between the two images. A filter that would more strongly emphasize individual samples (a high-frequency restoration filter, for example) may perform better than the classical high-pass filter, but this has yet to be confirmed.

Conclusions

The importance to be placed upon minimizing estimation error when reconstructing low-resolution data depends to a large extent on the image information of interest to the analyst. Whereas sample replication should be avoided in any reconstruction, it is not clear at this point whether the additional effort associated with co-kriging is warranted if textural information provides the main focus of the final interpretation task. In the many cases where geotechnical decisions rely on accurately reconstructing sample amplitudes, however, co-kriging provides the most flexible and accurate estimation procedure.

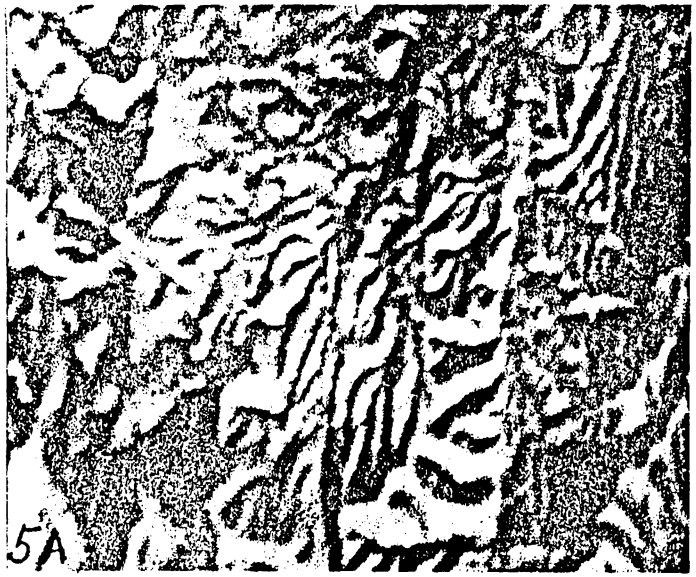

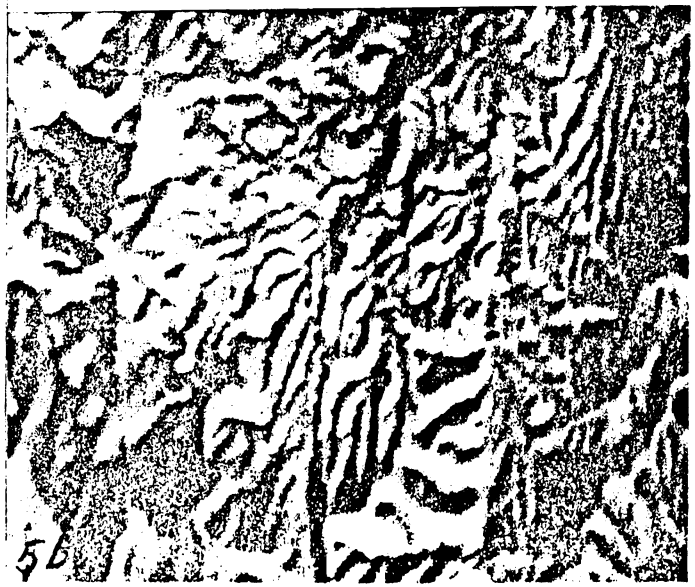

FIG. 5—*Reconstructed images. Figure* 5a *shows the kriged reconstructed image, and Fig.* 5b *shows an image reconstructed using simple sample replication.*

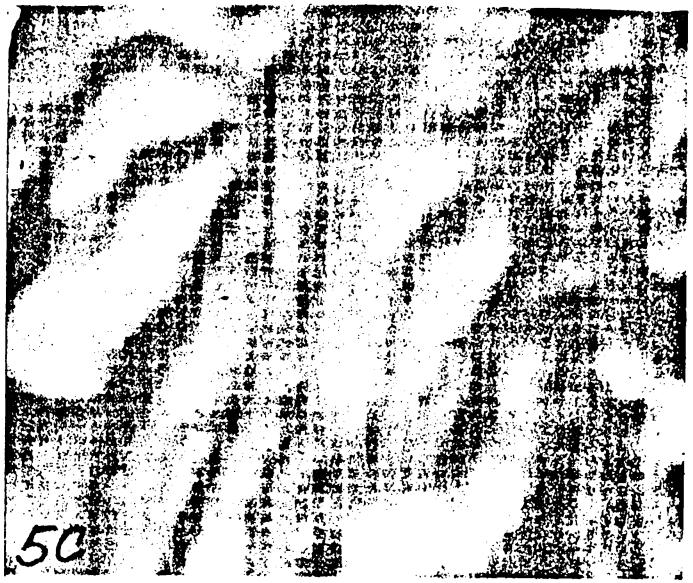

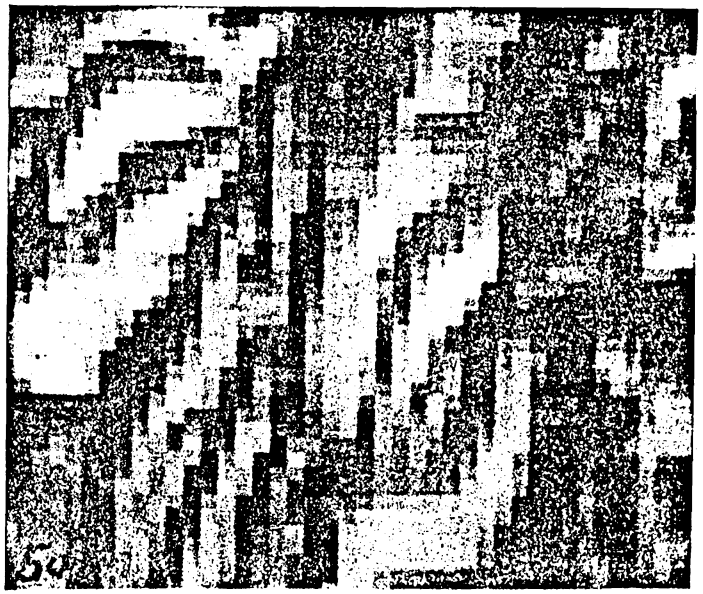

FIG. 5—*Continued: Figures* 5c *and* 5d *are enlargements of* 5a *and* 5b, *respectively.*

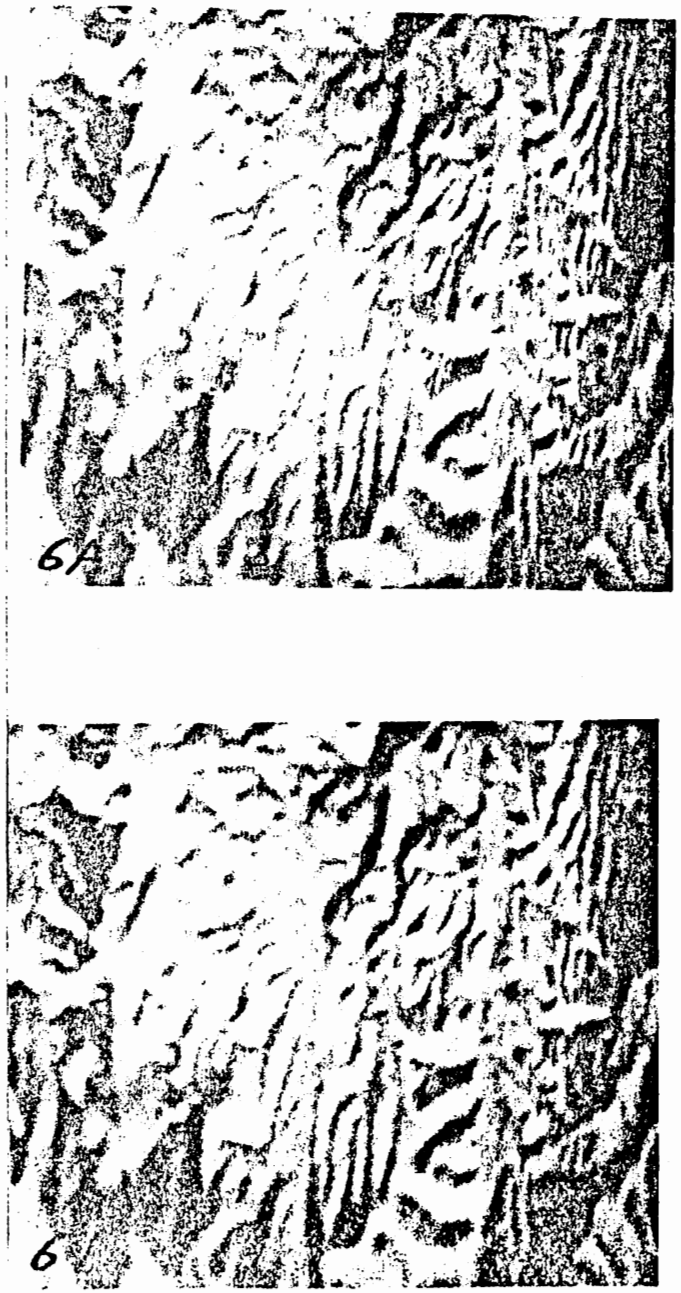

FIG. 6—*Contrast enhancement of Fig. 5a. In this figure the image in Fig. 5a has been enhanced using Eq 6, 6a and Eq 7, 6b. Note that Fig. 6a appears sharper than Fig. 5a.*

FIG. 7—*Texture enhancement of Fig. 5a. Figure 7 represents an increase in texture over Fig. 5a through addition of high frequencies from Fig. 2a. Although this image has more texture, the accuracy has been degraded as measured by the mean square error between Fig. 7 and Fig. 2b.*

Reconstructions produced in this preliminary experiment used global variogram functions (functions derived using entire images). Although this provides reasonable estimates, spatial characteristics may change throughout the image; the spatial correlation for a forest may differ from that for a desert. An approach that may improve the estimation involves computing variogram functions and estimating new samples within a moving window in a manner similar to spatial convolution. As pressure to automate image interpretation increases, co-estimation should become a standard image preprocessing tool.

References

[1] Sagi, D. and Julesz, B., *Science*, Vol. 228, 7 June 1985, pp. 1217-1219.
[2] Andrews, H. C. and Hunt, B. R., *Digital Image Restoration*, Prentice-Hall, Englewood Cliffs, NJ, 1977.
[3] Hartenstein, R., Wagner, G., Simons, D., and Coulson, J., "Image Interpolation With Dedicated Digital Hardware," *NASA Technical Briefs*, Fall 1985, p. 66.
[4] Schowengerdt, R. A., *Journal of Photogrammetric Engineering and Remote Sensing*, Vol. 46, No. 10, Oct. 1980, pp. 1325-1334.
[5] Steiner, D. and Salerno, A. E., "Remote Sensor Data Systems, Processing and Management," *Manual of Remote Sensing*, Reeves, Ed., American Society of Photogrammetry, Vol. 1, Chapter 4, 1975.
[6] Haralick, R. M., "Statistical and Structural Approaches to Texture," *Proceedings of the IEEE*, Vol. 67, No. 5, 1979, pp. 768-804.
[7] Matheron, G., *Economic Geology*, Vol. 58, 1963, pp. 1246-1266.
[8] Journel, A. G. and Huijbregts, C. J., *Mining Geostatistics*, Academic Press, New York, 1978, p. 253.
[9] Carr, J. R., Myers, D. E., and Glass, C. E., *Computers and Geosciences*, Vol. 2, No. 2, 1985, pp. 111-127.
[10] Myers, D. E., *Journal of Mathematical Geology*, Vol. 14, No. 3, 1982, pp. 249-257.
[11] Abrams, M. J., Brown, D., Lepley, L., and Sadowski, R., *Economic Geology*, Vol. 78, No. 4, 1983, pp. 591-604.

Q6329E
pd